# Supporting Information for "Using Tidally-Driven Elastic Strains to Infer Regional Variations in Crustal Thickness at Enceladus"

Alexander Berne[1], Mark Simons[1], James T. Keane[2], Ryan S. Park[2]

[1]California Institute of Technology, Pasadena, CA 91125 USA

[2]Jet Propulsion Laboratory, California Institute of Technology, Pasadena, CA 91109 USA

## Contents of this file

1. Text S1 to S2
2. Figures S1 to S3
3. Table S1

## Introduction

In S1, we outline our methodology for generating synthetic 'true' models of Enceladus's crust (1.1) and calculating the linear transfer function $\kappa(\mathbf{\Omega})$ in Equation 7 from the main text (1.2). In S2, we present the results of our iterative procedure for recovering crustal thickness using for a synthetic crustal model with a mean thickness $\tilde{D} = 50$ km (2.1).

## Text S1

### S1.1: Synthetic 'True' Crustal Thickness Model

To generate 'true' crustal thickness models (see Figures 2 and 3 of the main text), we first apply topography $H(\mathbf{\Omega})$ to the outer surface of spherically symmetric models.

Note that we can write $H(\mathbf{\Omega})$ as a sum over spherical harmonic basis functions scaled by coefficients $h_{lm}$:

$$H(\mathbf{\Omega}) = \sum_{l=0}^{\infty} \sum_{m=-l}^{l} h_{lm} Y_{lm}(\mathbf{\Omega}) \tag{1}$$

We extract $h_{lm}$ in Equation 1 for $l = 2 - 60$ from an updated version of topography at Enceladus using all available Cassini imagery (Park et al., personal communication). Our approach for inferring crustal thickness from strain is agnostic to the details of assumed topography. Details of the topography used in this study are therefore not important and are not intended to promote any particular model for Enceladus's shape. From $h_{lm}$, we generate components $d_{lm}^{true}$ in Equation 1 of the main text assuming a modified formulation for Airy-type compensation of surface topography (Hemingway & Matsuyama, 2017):

$$d_{lm}^{true} = h_{lm} + h_{lm} \frac{\rho_{ice}}{(\rho_w - \rho_{ice})} \frac{g}{g_{int}} \frac{R^2}{(R - \tilde{D})^2} (l-1)^{-N} \tag{2}$$

where $g_{int}$ is radial gravitational acceleration at the ice-ocean boundary, $\rho_{ice}$ is the mean density of the ice shell, and $\rho_w$ is the mean density of the ocean (see Table 1 of the main text for assumed parameter values), and $N$ is a dimensionless constant. Equation 2 demonstrates that the amplitude of variations in crustal thickness across $l$ depends on the chosen value of $N$. As $N$ decreases, the amplitude of variations in crustal thickness at large values of $l$ (i.e., short-wavelengths) increases rapidly. For models with $\tilde{D} = 25$ km, an assumed value of $N < 1.0$ produces negative (i.e., non-physical) crustal thickness near the South and North Poles. We aim to estimate the maximum extent short-wavelength variations in crustal thickness bias inferences of crustal thickness via gradient effects. We therefore generate a model with $N = 1.0$ for this work.

**S1.2: Computation of $\kappa(\mathbf{\Omega})$**

The quantity $\kappa(\mathbf{\Omega})$ is the linear transfer function which captures the sensitivity of strain fields to the angular position $\mathbf{\Omega}$ of crustal thickness variations in Enceladus's crust. We can approximate the impact of $\kappa(\mathbf{\Omega})$ by applying a high-pass filter $G$ to the ratio of the observed strain field $E^{obs}(\mathbf{\Omega})$ and $E^{Base}(\mathbf{\Omega})$:

$$\kappa(\mathbf{\Omega}) = \frac{E(\mathbf{\Omega})}{E^{Base}(\mathbf{\Omega})} \cdot \exp(G\left(\log\frac{E^{Base}(\mathbf{\Omega})}{E(\mathbf{\Omega})}\right)) \tag{3}$$

Note that we can write the log-ratio of $E^{obs}(\mathbf{\Omega})$ and $E^{Base}(\mathbf{\Omega})$ as a sum of spherical harmonics scaled by coefficients $\nu_{lm}$:

$$\log\frac{E^{Base}(\mathbf{\Omega})}{E^{obs}(\mathbf{\Omega})} = \sum_{l=0}^{\infty}\sum_{m=-l}^{l} \nu_{lm} Y_{lm}(\mathbf{\Omega}) \tag{4}$$

Because tidal forcing occurs at $l = 2$, we expect that the differential amount of $E(\mathbf{\Omega})$ produced by the location of thickness variations principally affects $\nu_{2m}$ and its first few harmonics (i.e., at even spherical harmonic degrees). We therefore designate the action of $G$ in Equation 4 to remove $\nu_{2m}$ (and its harmonics) from Equation 3 up to a maximum spherical harmonic degree $L'_{max}$:

$$\begin{aligned} &G\left(\sum_{l=0}^{\infty}\sum_{m=-l}^{l} \nu_{lm} Y_{lm}(\mathbf{\Omega})\right) \\ &\quad\to \sum_{l=0}^{\infty}\sum_{m=-l}^{l} \nu'_{lm} Y_{lm}(\mathbf{\Omega}) \quad \text{where} \quad \begin{cases} \nu'_{lm} = 0, & \text{if } l \,\%\, 2 = 0 \text{ and } l \leq L'_{max} \\ \nu'_{lm} = \nu_{lm}, & \text{otherwise} \end{cases} \end{aligned} \tag{5}$$

For this work, we set $L'_{max} = 4$; however, we find that our selection of $L'_{max}$ does not significantly impact final results for $L'_{max} = 4 - -10$ following the iterative procedure described in section 3.2 in the main text.

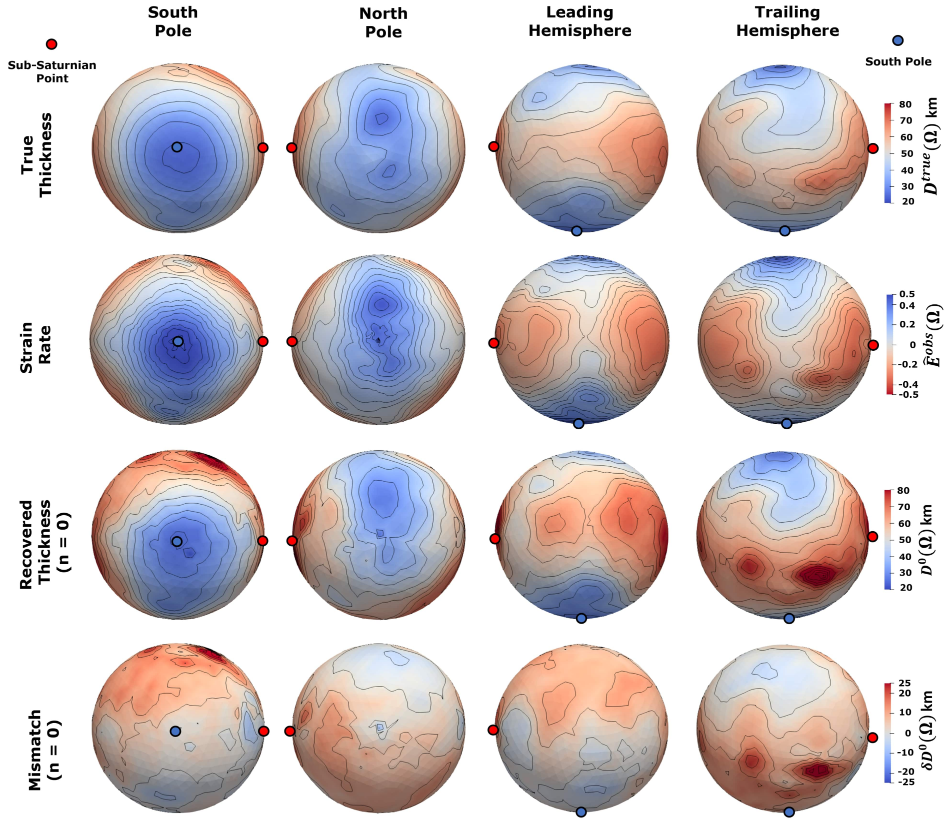


**Figure S1.** Similar to Figure 2 of the main text except $\tilde{D} = 50$ km for 'true' models.

## Text S2

### S2.1: Results for model with $\tilde{D} = 50$ km

We reproduce Figures 2, 3, and 4 (i.e., Figures S1, S2, and S3) using for a synthetic crustal model with a mean thickness $\tilde{D} = 50$ km.

## References

Hemingway, & Matsuyama, I. (2017). Isostatic equilibrium in spherical coordinates and implications for crustal thickness on the Moon, Mars, Enceladus, and elsewhere. *Geophysical Research Letters*, *44*(15). doi: 10.1002/2017GL073334

Iess, L., Stevenson, D. J., Parisi, M., Hemingway, D., Jacobson, R. A., Lunine, J. I., & Tortora,

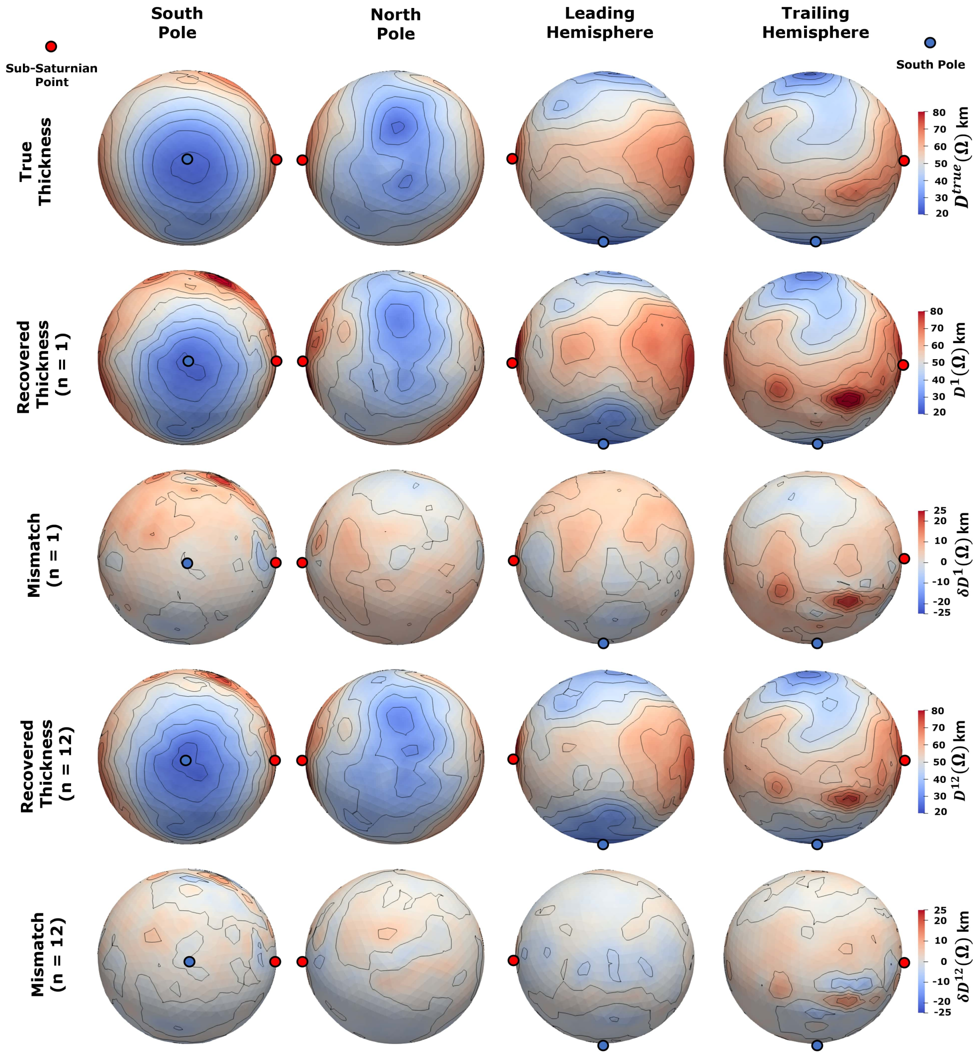


**Figure S2.** Similar to Figure 3 of the main text except $\tilde{D} = 50$ km for 'true' models

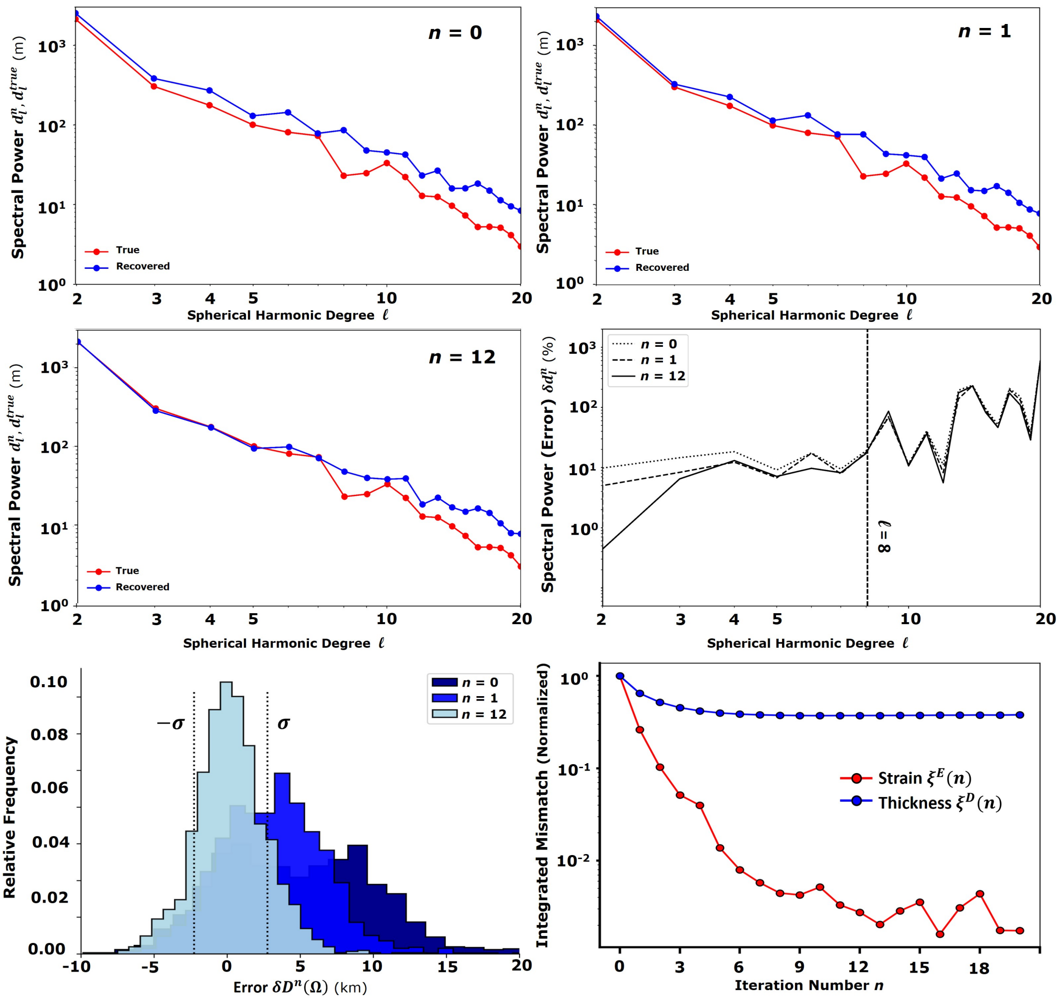


**Figure S3.** Similar to Figure 4 of the main text except $\tilde{D} = 50$ km for 'true' models and lower right panel shows the cost function and integrated thickness mismatch (normalized relative to the maximum value) for iterations $n = 0 - 20$. Vertical dash-dot line at $l = 8$ marked for reference in center right panel.

**Table S1.** Assumed values for parameters used throughout this work. Parameter values extracted from Schenk et al., (2018); Iess et al., (2014); and Souček et al., (2016).

| **Parameter** | **Value** | **Units** |
|---|---|---|
| $R$ | 252.1 | km |
| $\tilde{D}$ | 25.0 | km |
| $G$ | 3.3 | GPa |
| $\mu$ | 8.6 | GPa |
| $\rho_{ice}$ | 925 | kg/m$^3$ |
| $\rho_w$ | 1007 | kg/m$^3$ |
| $g$ | 0.113 | m/s$^2$ |
| $g_{int}$ | 0.120 | m/s$^2$ |
| $e$ | 0.0047 | N/A |
| $\omega$ | $5.307 \cdot 10^{-5}$ | s$^{-1}$ |

P. (2014). The gravity field and interior structure of Enceladus. *Science*, *344*(6179). doi: 10.1126/science.1250551

Schenk, P. M., Clark, R. N., Howett, C. J. A., Verbiscer, A. J., & Waite, J. H. (2018). *Enceladus and the icy moons of saturn.* doi: 10.2458/azu_uapress_9780816537075

Souček, O., Hron, J., Běhounková, M., & Čadek, O. (2016). Effect of the tiger stripes on the deformation of Saturn's moon Enceladus. *Geophysical Research Letters*, *43*(14). doi: 10.1002/2016GL069415